[10] J. C. Pedro and N. B. Carvalho, "A very fast and efficient computation method for nonlinear distortion on uniformly discretized spectra," in *Proc. Telecommun. Conf. II* , 1999, pp. 519–522.

[11] J. A. García, J. C. Pedro, M. L. De la Fuente, N. B. Carvalho, A. Mediavilla, and A. Tazón, "Resistive FET mixer conversion loss and IMD optimization by selective drain bias," *IEEE Trans. Microwave Theory Tech.*, vol. 47, pp. 2382–2392, Dec. 1999.

# Uniplanar One-Dimensional Photonic-Bandgap Structures and Resonators

Tae-Yeoul Yun and Kai Chang

***Abstract*—This paper presents uniplanar one-dimensional (1-D) periodical structures, so-called photonic-bandgap (PBG) structures, and defect high-$Q$ resonators for coplanar waveguide, coplanar strip line, and slot line. Proposed uniplanar PBG structures consist of 1-D periodically etched slots along a transmission line or alternating characteristic impedance series with wide band-stop filter characteristics. A stop bandwidth obtained is 2.8 GHz with a stopband rejection of 36.5 dB. This PBG performance can be easily improved if the number of cells or the filling factor is modified in a parametric analysis. Using uniplanar 1-D PBG structures, we demonstrate new high-$Q$ defect resonators with full-wave simulation and measured results. These structures based on defect cavity or Fabry–Perot resonators consist of a center resonant line with two sides of PBG reflectors. They achieve a loaded $Q$ of 247.3 and unloaded $Q$ of 299.1. The proposed circuits should have many applications in monolithic and hybrid microwave integrated circuits.**

***Index Terms*—Band-stop filter, photonic bandgap, resonator, uniplanar.**

## I. Introduction

Similarly to the energy bandgap concept in solid-state electronic materials, photonic-bandgap (PBG) materials or photonic crystals provide a means to control lightwave propagation. Although the PBG structure was developed for use at optical frequencies, it is scalable to microwave and millimeter-wave frequencies because the PBG is an electromagnetic bandgap (EBG) [1]. A one-dimensional (1-D) PBG structure can be made by alternating wave impedances, which has been analyzed and applied to several transmission lines and waveguides in microwave engineering to demonstrate stopband and slow-wave characteristics [2]. In this paper, however, the periodicity is referred to as the PBG because ideas of a new 1-D resonator are based on the defect cavity concept [1].

Two-dimensional (2-D) PBG structures published for antenna and microstrip-line applications consisted of periodical air holes, which are micromachined or drilled through the substrate [3], [4]. A most recently reported 2-D PBG structure for microstrip lines was composed of circularly etched holes on the ground plane along the microstrip line without drilling [5]. The periodically etched hole technique avoids the drilling process and makes PBG structures easier to manufacture. Since most electromagnetic fields are confined to the microstrip-line width, 2-D hole structures can be modified to 1-D structures. In addition, use of uniplanar structures has an advantage that only a one-sided photolithography process is required. In this paper, uniplanar 1-D PBG structures for a coplanar waveguide (CPW), coplanar strip line (CPS), and slot-line PBG are designed, as shown in Fig. 1(a).

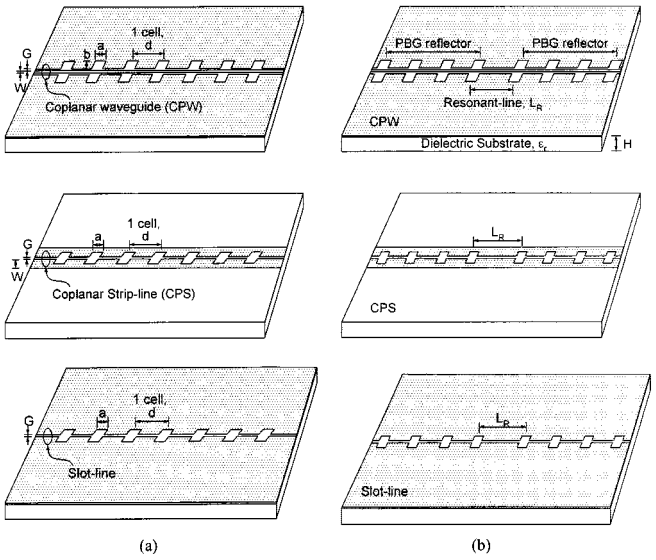


Fig. 1. Uniplanar (CPW, CPS, and slot line) 1-D periodical structures. (a) 1-D PBG bandstop filters. (b) 1-D PBG resonators.

Using the defect cavity concept, 1-D or 2-D optical waveguide resonators with an alternating dielectric constant [6], [7] and image guide resonator [8] have been published for high quality ($Q$) resonators. Fig. 1(b) shows new CPW, CPS, and slot-line uniplanar resonators using 1-D PBG structures [9]. These resonators consist of a center resonant-line (defect) with periodic PBG reflectors on both sides to implement Fabry–Perot resonators. Two important parameters are analyzed and full-wave simulation and measured results are presented. The uniplanar defect resonators can be readily implemented in monolithic microwave integrated circuits (MMICs) in which loss compensation circuits with active devices can be used.

## II. Design and Parametric Analysis

The PBG structure is basically a periodical structure that satisfies the following equation, and strongly shows band-stop filter characteristics as the number of cells is increased [1]:

$$k = \frac{\pi}{d} \tag{1}$$

where $k$ is the propagation constant. The cell distance ($d$) is equal to 1/2 guided wavelength ($\lambda_g$) if $k$ is equal to $2\pi/\lambda_g$. The propagation constant is difficult to determine and full-wave analysis is necessary to calculate $\lambda_g$ for the structures in Fig. 1. As a simple approximation, it is acceptable to set the propagation constant as approximately the same as an unperturbed transmission line, assuming that the perturbation of the PBG structure is very small [5]. The circuit length is dependent on the cell number, center frequency, and dielectric constant. In this study, the substrate used is a RT/Duroid 6010.5, with relative dielectric constant ($\varepsilon_r$) of 10.5, height ($H$) of 50 mil, and length of 2 in. The stopband center or resonant frequency ($f_o$) is chosen near 10 GHz and, thus, the

Manuscript received September 7, 1999. This work was supported in part by the State of Texas Higher Education Coordinating Board under their Advanced Technology Program.

The authors are with the Department of Electrical Engineering, Texas A&M University, College Station, TX 77843-3128 USA (e-mail: tyyun@ee.tamu.edu; chang@ee.tamu.edu).

Publisher Item Identifier S 0018-9480(01)01692-1.

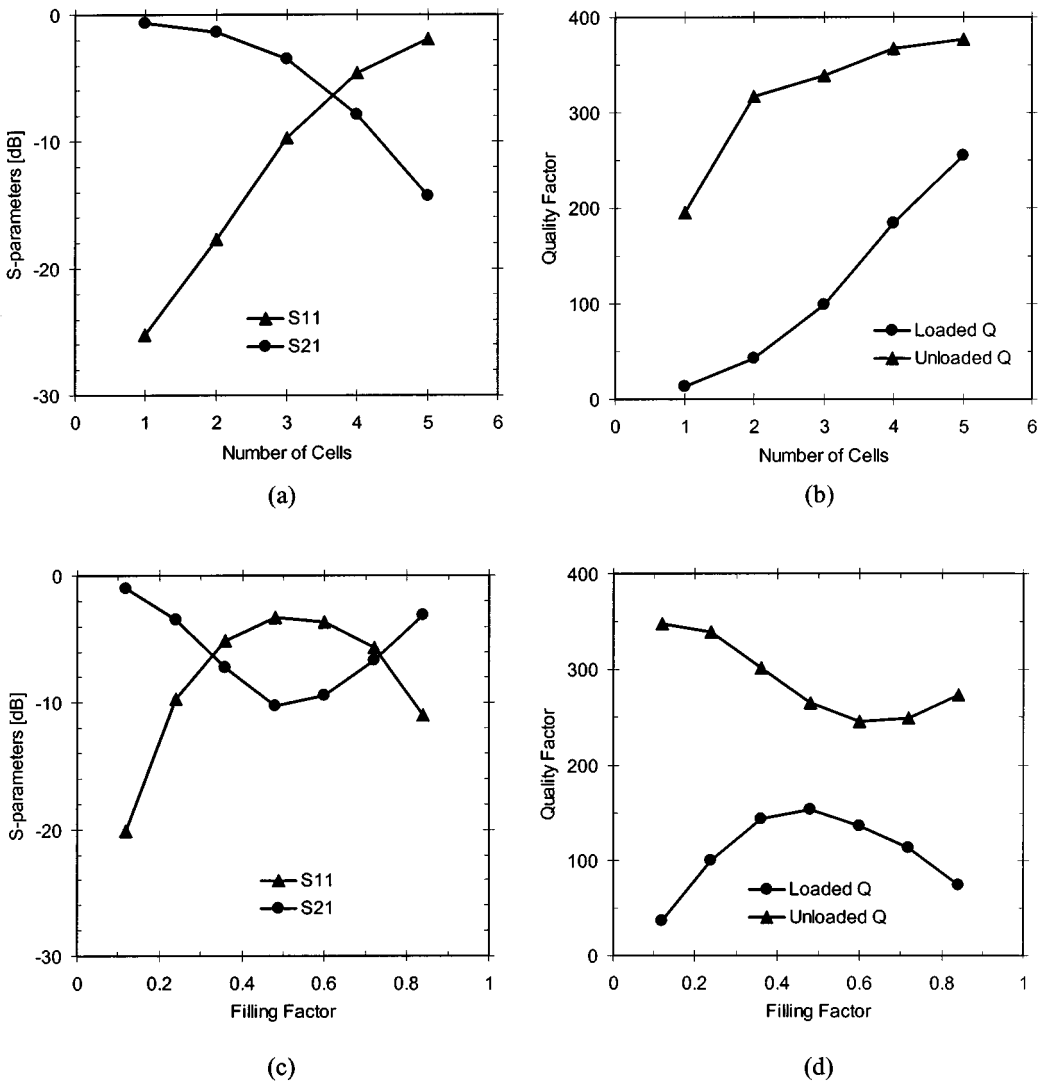


Fig. 2. Effects of design parameters on CPW PBG resonator characteristics. (a) $S$-parameters versus the number of cells. (b) $Q$-factors ($Q_L$, $Q_U$) versus the number of cells with $a/d = 60/250$. (c) $S$-parameters versus filling factor. (d) $Q$-factors versus filling factor with $b$ of 60 mil and three cells.

distance of cells is about 250 mil for $\lambda_g/2$ and the number of cells is seven.

There are three PBG design variables: size ($a$, $b$), distance ($d$), and number of cells in Fig. 1. As described above, the center frequency ($f_o$) of the PBG stopband is related with the cell distance of $\lambda_g/2$ [1]. The hole size and number of cells affect the stopbandwidth ($\mathrm{BW}_{-20\ \mathrm{dB}}$), stopband rejection, ripples of passband insertion loss ($S_{21}$), and return loss ($S_{11}$) bouncing magnitude. The PBG structure shows the EBG or band-rejection characteristics. The prohibition of wave propagation in the forbidden gap makes the periodic structure valuable as a reflector. Microwaves are bounced back and forth within a defect cavity or a resonant transmission line, which is sandwiched between two PBG reflectors forming a Fabry–Perot resonator. Fig. 1(b) shows uniplanar defect resonators consisting of a resonant-line length ($L_R$) of $1.5d$ with a PBG reflector of three cells on each side.

A parameteric analysis was carried out for uniplanar 1-D PBG resonators. Fig. 2 shows results of $S$-parameters and quality factors versus the filling factor ($a/d$) and the number of cells. Fixed parameters of the CPW defect resonator are a strip width ($W$) of 16.4 mil, a gap ($G$) of 10 mil, a size ($b$) of 60 mil, and a resonant-line length ($L_R$) of 375 mil ($= 1.5d$). All simulation results are achieved using Zeland Software's IE3D and Fidelity. Full-wave simulators are essential in PBG analysis and design because of high complexity. The unloaded $Q$-factor ($Q_U$) is calculated from the loaded $Q$-factor ($Q_L$) and a resonator loss ($L$), which excludes a mismatch loss and a suminiature A (SMA) connection loss (1.2 dB at 10 GHz). $Q_U$ and $Q_L$ are given by

$$Q_U = \frac{Q_L}{1 - 10^{L/20}} \tag{2}$$

$$Q_L = \frac{f_c}{\Delta f_{3\ \mathrm{dB}}} \tag{3}$$

$$\text{Resonator loss } (L) = |S_{21}| - |\text{Mismatch loss}| - |\text{SMA connection loss}| \tag{4}$$

$$\text{Mismatch loss [dB]} = 10\log_{10}(1 - |S_{11}|^2) \tag{5}$$

$$\text{SMA connection loss [dB]} = |MS_{21}| - |SS_{21}| \tag{6}$$

where $f_c$ is the resonant center frequency, $\Delta f_{3\ \mathrm{dB}}$ is the $-3$-dB bandwidth, $|MS_{21}|$ is a measured $|S_{21}|$ for a 50-$\Omega$ line with an SMA connection, and $|SS_{21}|$ is a full-wave simulated $|S_{21}|$ for a 50-$\Omega$ line without an SMA connection [8], [10].

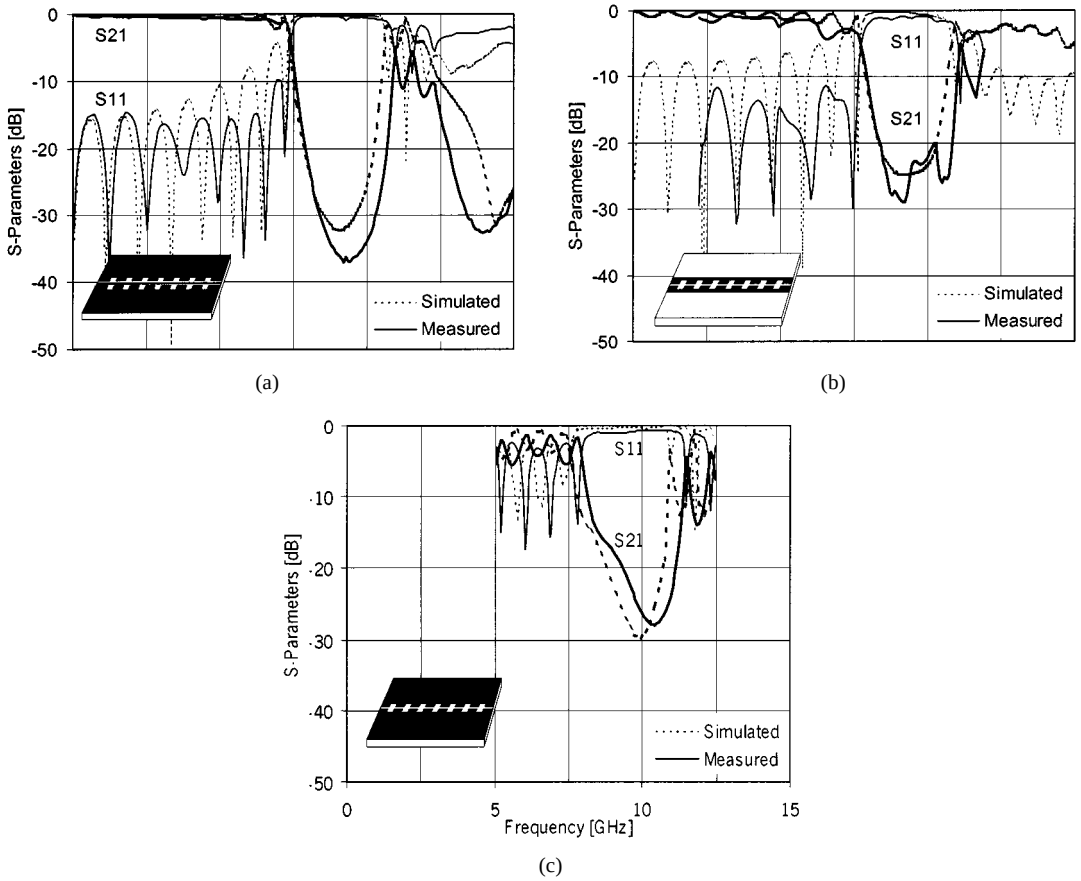


Fig. 3. Simulated and measured results for uniplanar 1-D periodical structures of band-stop filters. (a) CPW. (b) CPS. (c) Slot-line.

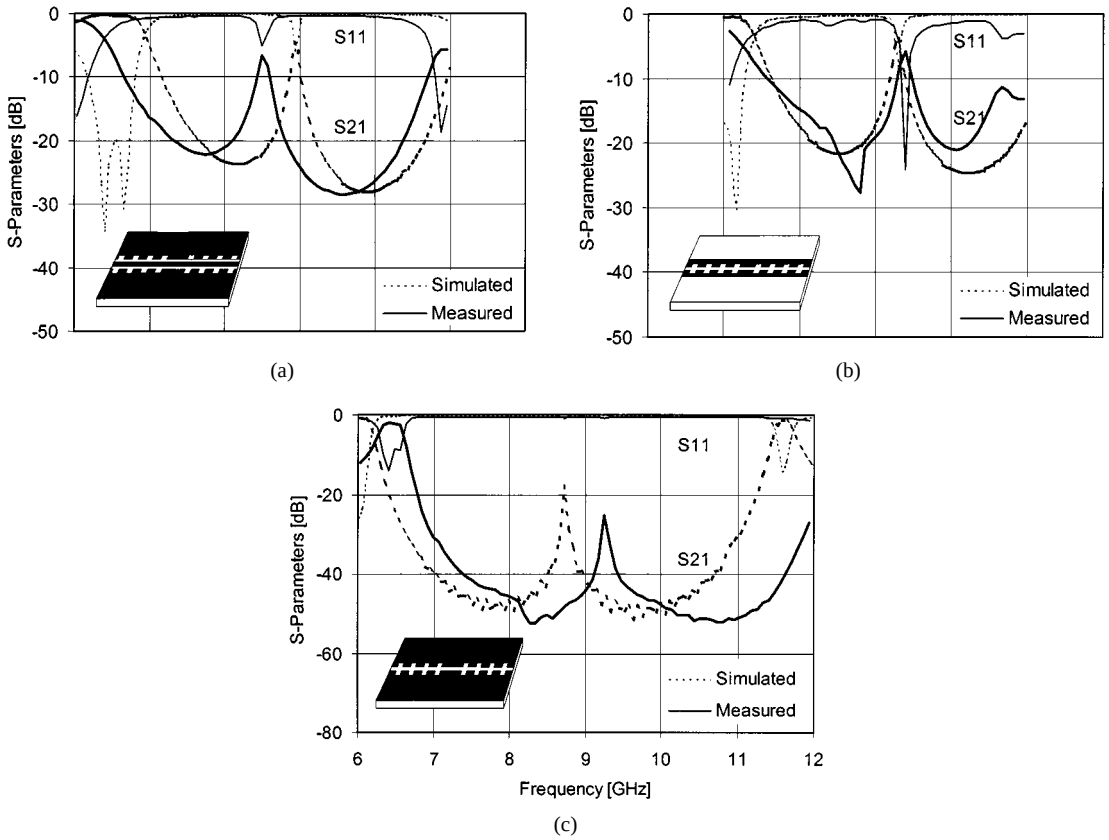


Fig. 4. Simulated and measured results for resonators with uniplanar 1-D PBG reflectors. (a) CPW. (b) CPS. (c) slot line.

TABLE I
DESIGN PARAMETERS AND MEASURED RESULTS FOR UNIPLANAR 1-D PBG BAND-STOP FILTERS WITH $a = b$

| Structure | Design Parameters | | $f_o$ [GHz] | Stop $BW_{-20dB}$ [GHz] | Stopband Rejection [dB] |
|---|---|---|---|---|---|
| | $W$[mil] / $G$[mil] / No. of cell | Filling Factor ($a$[mil]/$d$[mil]) | | | |
| CPW | 16.4 / 10 / 7 | 60/250 = 0.24 | 9.3 | 2.8 | -36.5 |
| CPS | 63 / 6 / 7 | 30/250 = 0.12 | 9.7 | 2.5 | -25.0 |
| Slot | NA / 6 / 7 | 30/250 = 0.12 | 9.7 | 1.9 | -23.5 |

TABLE II
DESIGN PARAMETERS AND MEASURED RESULTS FOR UNIPLANAR 1-D PBG RESONATORS WITH $a = b$

| Structure | Design Parameters | | $Q_L$ | $Q_U$ | $f_c$ [GHz] | $S_{21}$ [dB] | $S_{11}$ [dB] |
|---|---|---|---|---|---|---|---|
| | $W$[mil] / $G$[mil] / No. of cell | Filling Factor ($a$[mil]/$d$[mil]) | | | | | |
| CPW | 16.4 / 10 / 3 | 60/250=0.24 | 67.0 | 193.2 | 8.5 | -5.9 | -6.8 |
| CPS | 63 / 6 / 3 | 30/250=0.12 | 51.4 | 226.0 | 9.3 | -3.6 | -14.4 |
| Slot | NA / 6 / 3 | 50/250=0.20 | 247.3 | 299.1 | 9.3 | -22.6 | -1.2 |

For the CPW defect resonator in Fig. 2, two design parameters of cell numbers and filling factors ($a/d$) are varied. In Fig. 2(a), as the number of cell is increased, $S$-parameter ($S_{11}$, $S_{21}$) performance is degraded because of increasing reflecting and leaking energy. In Fig. 2(b), as the number of cells increases, $Q_L$ increases and is close to $Q_U$, which is nearly constant with a large number of cells. The reason of the unvarying $Q_U$, even though the leakage loss increased with a larger number of cells, may be explained as follows. The increasing number of cell confines the energy closer to the resonant-line area and, thus, the metal and dielectric loss is reduced. This means that $Q_U$ increases. However, the increased energy leakage via slots or cells makes $Q_U$ lower. Finally, $Q_U$ factor reaches constant. This estimate was confirmed with an electromagnetic field distribution with IE3D. In Fig. 2(c) and (d), there is an optimum filling factor of about 0.5 for $Q_L$, at which filling factor $Q_U$ is close to the minimum because of the large leakage. This large leakage degrades $S$-parameter performance, which is a tradeoff with the optimum $Q_L$. As a result, the larger is the number of cells, the larger is the $Q_L$. However, the $Q_L$ is limited by $Q_U$. In addition, the increase in the filling factor will not always improve $Q_L$ and there is an optimum value. Similar analysis has been performed for uniplanar PBG band-stop filters. The larger the number of cells, the wider the stopbandwidth, and the higher the stopband rejection. However, there is an optimum filling factor near 0.5–0.6.

## III. EXPERIMENTS

Uniplanar 1-D PBG band-stop filters, shown in Fig. 1(a), are simulated and measured, as shown in Fig. 3. Scattering parameters $S_{11}$ and $S_{21}$ are measured using a Hewlett-Packard HP8510B network analyzer. Design parameters and measured results are summarized in Table I. Measured bandwidth ($\mathrm{BW}_{-20\ \mathrm{dB}}$), center frequency ($f_o$), and magnitude of the measured $S_{11}$ and $S_{21}$ agree very well with the prediction. Seven bounces in the $S_{11}$ response are shown corresponding to seven cells. As a result, the 1-D uniplanar PBG structures using etched slots or alternating $Z_c$ series have achieved a stop bandwidth of 20%–30% and a stopband rejection from $-23.5$ to $-36.5$ dB. Described in the above parametric analysis, these band-stop characteristics can be improved if the number of cells increases or the filling factor ($a/d$) is optimized. Uniplanar 1-D PBG defect resonators in Fig. 1(b) are designed with a resonant-line length ($L_R$) of 375 mil ($= 1.5d$) and cell number of three. Other design parameters and measured results of Fig. 4 are summarized in Table II. Measured and simulated results agree fairly well, except that the resonant frequency ($f_o$) is shifted by $\pm 0.4$ GHz or $\pm 4.4\%$. This difference is mainly caused by nonsimulated effects of test fixture parasitic, copper thickness, and etching tolerance. A high $Q_L$ of 247.3 and $Q_U$ of 299.1 were achieved from the slot-line defect resonator.

## IV. CONCLUSION

In conclusion, new uniplanar 1-D PBG band-stop filters and resonators have been demonstrated to achieve wide stopbandwidth and high $Q$-factor. The relationship between the filling factor or the number of cells and the bandwidth, stopband rejection, or $Q$-factor has been studied. Measured data agree very well with theoretical electromagnetic simulated results. Results of this paper should have many applications for microwave integrated circuits and antennas.

## ACKNOWLEDGMENT

The authors would like to thank M.-Y. Li, Texas A&M University, College Station, for technical assistance, and H. Tehrani, Texas A&M University, College Station, P. Zepeda, Texas A&M University, College Station, and J. Guill, Texas A&M University, College Station, for incentives and invaluable discussions.

## REFERENCES

[1] J. D. Joannopoulos, R. D. Meade, and J. N. Winn, *Photonic Crystals: Molding the Flow of Light*. Princeton, NJ: Princeton Univ. Press, 1995.
[2] R. E. Collin, *Foundations for Microwave Engineering*, 2nd ed. New York: McGraw-Hill, 1992, ch. 8.
[3] T. J. Ellis and G. M. Rebeiz, "Millimeter-wave tapered slot antennas on micromachined photonic bandgap dielectrics," in *IEEE MTT-S Int. Microwave Symp. Dig.*, San Francisco, CA, June 1996, pp. 1157–1160.
[4] Y. Qian, V. Radisic, and T. Itoh, "Simulation and experiment of photonic band-gap structures for microstrip circuits," in *Proc. Asia–Pacific Microwave Conf.*, Hong Kong, Dec. 1997, pp. 585–588.

[5] V. Radisic, Y. Qian, R. Coccioli, and T. Itoh, "Novel 2-D photonic bandgap structure for microstrip lines," *IEEE Microwave Guided Wave Lett.*, vol. 8, pp. 69–71, Feb. 1998.
[6] J. S. Foresi *et al.*, "Photonic-bandgap microcavities in optical waveguides," *Nature*, vol. 390, pp. 143–145, 1997.
[7] D. Lailloy *et al.*, "Demonstration of cavity mode between two-dimensional photonic-crystal mirrors," *Electron. Lett.*, vol. 33, no. 23, pp. 1978–1979, Nov. 1997.
[8] F.-R. Yang, Y. Qian, and T. Itoh, "A novel high-$Q$ guide resonator using band-gap structures," in *IEEE MTT-S Int. Microwave Symp. Dig.*, Baltimore, MD, June 1998, pp. 1803–1806.
[9] T. Y. Yun and K. Chang, "One-dimensional photonic bandgap resonators and varactor tuned resonators," in *IEEE MTT-S Int. Microwave Symp. Dig.*, Anaheim, CA, June 1999, pp. 1629–1632.
[10] K. Chang, *Microwave Ring Circuits and Antennas*. New York: Wiley, 1996.

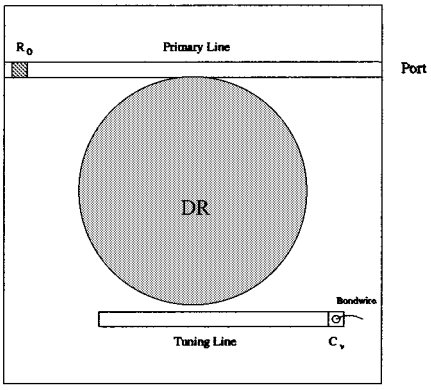


Fig. 1. DR in cavity, with microstrip lines and varactor.

## Improved Tuning Prediction for the Microstrip Coupled Dielectric Resonator Using Distributed Coupling

Xiaoming Xu and Robin Sloan

***Abstract*—In this paper, accurate modeling of the varactor-tuned dielectric resonator (DR) using distributed coupling between the DR and microstrip lines is investigated on the basis of three-dimensional electromagnetic study. The magnetic coupling between the DR and microstrip line is appreciable over a length greater than the diameter of the DR. The distribution of this coupling should be considered when calculating the electronic frequency tuning range. A novel circuit model is introduced to represent the coupling as distributed, with an integral method to calculate equivalent-circuit parameters efficiently. The distributed model provides much better accuracy than the conventional lumped model [1]–[3]. A comparison is made between the calculated tuning range of 23 MHz achieved by the distributed model, which agrees closely with a measurement of 20.2 MHz, and that of 89 MHz predicted by the conventional lumped model. The circuit model of distributed coupling is, therefore, valuable in the design of DR oscillators.**

***Index Terms*—Dielectric resonator, distributed coupling, tuning range, varactor tuning.**

### I. Introduction

Dielectric resonators (DRs) are commonly used as stabilization elements in oscillators [4]. The high quality factors realizable with the DR yield a relatively low oscillator phase noise. The most common oscillator configuration is the reflection mode with the DR located off a microstrip line attached to the active device. The electromagnetic (EM) mode employed, most commonly the $\mathrm{TE}_{01\delta}$ mode, may be tuned electronically using a varactor diode mounted on an adjacent transmission line, as shown in Fig. 1. Usually, the desired oscillation frequency is maintained by electronically compensating for temperature drift, but could also be required to maintain phase lock to a reference oscillation. In their paper [3], Buer and El-Sharawy discussed the importance of using a nonresonant varactor tuning line and applied the lumped equivalent circuit. Resonance in the varactor tuning line should be avoided or else spurious oscillations and undesirable frequency hopping can occur.

Manuscript received September 17, 1999. This work was supported by the Engineering and Physical Sciences Research Council under Contract GR/K78744.

The authors are with the Department of Electrical Engineering and Electronics, University of Manchester Institute of Science and Technology, Manchester M60 1QD, U.K.

Publisher Item Identifier S 0018-9480(01)01693-3.

Modeling the DR circuit traditionally relies upon deriving a lumped equivalent circuit based upon curve fitting the response to either directly measured or electromagnetically simulated $S$-parameters [1]–[3]. In this paper, a more accurate alternative model is expounded, which is capable of accurately predicting the achievable tuning range. Compared with the classic lumped equivalent circuit, the distribution of coupling between a DR and a microstrip line is modeled by the mutual inductance of multiple sections. Parameters of the equivalent model are derived through the integration of the appropriate EM-field component and, thus, the model is truly representative of the actual EM fields. Komatsu and Murakami [5] have also calculated the coupling to the DR based on EM-field distribution. However, the magnetic field is then integrated along the microstrip line to yield an overall lumped coupling. For the results presented here, the EM-field distribution is generated for a single frequency point corresponding to peak energy storage at the $\mathrm{TE}_{01\delta}$-mode resonance eigenfrequency. This is computationally efficient, requiring only a single simulation with corresponding post-processing to yield the equivalent distributed circuit components. These components are then applied to a nodal simulation package such as HP EEsof's Libra, thus yielding the $S$-parameter response rapidly. It is then far quicker to optimize parameters of this equivalent circuit than the dimensions of the three-dimensional EM model. The approach is general enough to be applied to any DR coupled circuit comprising one or more transmission lines.

### II. Distribution of Coupling and Circuit Model

Conventional circuit models for a DR coupling to a microstrip line are based on the assumption that the coupling between the DR and microstrip line is concentrated at the middle of the line. A three-dimensional field study reveals that the coupling component of the magnetic field spreads widely along the line as described in [1].

Using nodal analysis software, such as Libra, mutual inductances are used to represent the distribution of magnetic coupling between the DR and microstrip lines. The microstrip lines are divided into short sections of 0.5 mm ($\lambda/27$). The total inductance of the DR, i.e., $L_r$, is distributed on the secondary side of the inductors. For convenience, an additional inductance, i.e., $L_a$, is introduced to take account of the remainder as follows:

$$L_r = \sum L_t + L_a \tag{1}$$

where $L_t$ is the microstrip inductance in each section.